Embedding of Nanoscale 3D SiGe Islands in a Si Matrix

P. Sutter and M. G. Lagally
University of Wisconsin—Madison, Madison, Wisconsin 53706
(Received 28 May 1998)

The epitaxial embedding of faceted three-dimensional SiGe islands in a Si matrix has been investigated by low-energy electron microscopy. Under a Si flux these islands expand and undergo a shape change to incorporate a (100) top facet. A physical interpretation of the atomistic mechanism producing the shape change is presented and supported with a simple model. [S0031-9007(98)07384-0]

PACS numbers: 68.35.Bs, 61.16.Bg

Modern techniques of epitaxial growth make possible the synthesis of planar semiconductor films with monolayer thickness control. Because of the increasing interest in quantum wires and dots for potential future semiconductor electronic devices, much effort has been devoted recently to extending this capability to the formation of structures with nanometer size in two or three dimensions. Many systems in which film and substrate materials have the same crystal structure but differ somewhat in their lattice constants naturally form nanoscale three-dimensional (3D) islands: Growth of a planar film, strained to the in-plane lattice constant of the substrate, breaks down at some layer thickness, and additional deposition leads to the formation of 3D islands on top of this wetting layer [1] that are coherently matched to the underlying lattice. Through refined choice of material and growth parameters, ordered arrays of uniformly sized, faceted nanoscale islands can be achieved by such self-assembly [2]. The resulting ensembles of electronically coupled islands promise to become useful building blocks in future electronic devices and represent a unique arena for fundamental investigations.

For measurements of basic electronic properties as well as for device applications, it is necessary to create buried quantum dots by embedding such nanostructures in a matrix. Such epitaxial embedding yields an excellent passivation of the dot surface, resulting in a predictable intrinsic potential profile within the quantum dot itself and in a well-defined potential barrier between the dot and the surrounding matrix. However, embedding can also complicate predictions of the electronic structure of real samples. Apart from producing inhomogeneous strain due to the lattice mismatch between the dot and barrier materials, which is usually accounted for in electronic structure calculations, embedding can change the composition and the shape of the dots, both of which significantly affect their band structure [3].

Despite its importance, the embedding of self-assembled quantum dots has not been studied systematically [2,4], and obvious shape changes of buried islands have been ignored until quite recently [5,6]. In the SiGe system, for example, transmission electron microscopy (TEM) images show that overgrowth transforms pyramidal islands into truncated pyramids [5] of reduced height. The physical mechanisms driving these shape transitions are, however, unknown. In this Letter we describe the embedding of 3D SiGe hut islands using real-time low-energy electron microscopy (LEEM) observations of the morphological evolution of such islands as Si is deposited on them. We provide a detailed discussion of the physical mechanisms governing the observed shape changes. We suggest that the mechanisms found here are generally applicable to systems exhibiting lattice stress driven self-assembling 3D island growth.

Growth experiments were performed in the LEEM on (100) oriented Si substrates using Si_2H_6 and Ge_2H_6. In a first step, the surface was seeded with an array of coherent islands by depositing a $Si_{1-x}Ge_x$ alloy ($x \sim 0.4$) at 750 °C [7]. The alloy coverage was chosen to yield pyramid-shaped (105) faceted hut islands [8] coexisting with somewhat larger, dome-shaped multifaceted islands [8,9] to detect possible modifications in the embedding that depend on initial island shape. Following SiGe alloy growth, the sample temperature was lowered to 650 °C and Si was deposited at a rate of 2.3 monolayers (ML) per minute to embed the islands and gradually recover a flat surface. LEEM images were recorded during deposition in bright-field mode, using electrons specularly reflected from the sample surface. Imaging conditions, chosen such that large planar areas with (100) orientation appear bright while facets with oblique surface normals and groups of closely spaced steps appear dark, allow us to measure quantitatively the (100) projected size of individual 3D islands, during their initial formation as well as during their subsequent embedding in Si. Additional island height information was obtained by cross-sectional transmission electron microscopy (XTEM) on some of the samples.

Figure 1 shows a sequence of LEEM images illustrating the evolution of island morphology with increasing Si coverage at a temperature of 650 °C. Dark spots mark the base area of individual islands, most of which are coherent (105) faceted huts [10]. These huts are strained at their base to the Si lattice constant, and partially relax the strain toward their top [11], but must be throughout under compressive stress to maintain the (105) facets. If

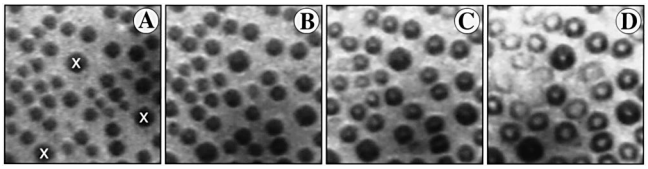

FIG. 1. Sequence of LEEM images, taken at $T = 650$ °C and a deposition rate of 2.3 ML/min, illustrating the overgrowth of 3D SiGe islands. (A) SiGe islands prior to Si deposition. Most of the islands are (105) faceted huts, which appear somewhat rounded at this elevated temperature. Three larger, multifaceted dome islands are also present (marked "*X*"). (B), (C), and (D) Islands during Si deposition, at 4.6, 9.2, and 13.8 ML coverage, respectively. Field of view: $1.5 \times 1.5\ \mu m^2$.

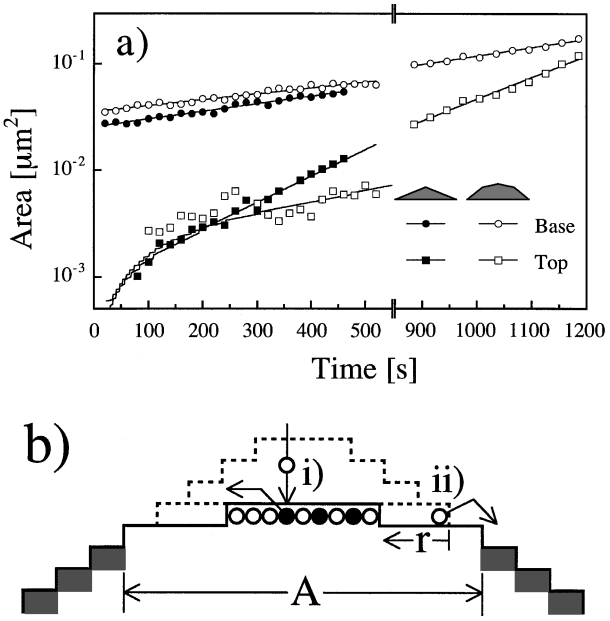

FIG. 2. Shape change of 3D SiGe islands during embedding in Si. (a) Evolution of the projected island geometry as a function of Si deposition time. Points indicate experimental values measured from sequences of LEEM images, recorded in real time during Si growth. Lines show the results of model calculations on the formation and expansion of a (100) facet at the island apex (bottom), and the increase of the base area (top). (b) Illustration of the model for the island apex dissolution. Layer-by-layer dissolution is driven by incorporation of Si (i), followed by atom detachment from the topmost terrace (ii), whose area thus decreases at a rate r. Bright-field LEEM detects the area "*A*" as a bright spot surrounded by dark contrast from the adjacent facets.

that were not the case, the 3D islands would form a (100) top surface. The shape of the huts projected onto (100) is not perfectly square but somewhat rounded at this elevated temperature, probably due to thermal rounding of the edges between adjacent facets. Because of their low Ge content most of the hut islands are quite large, with a base dimension of about 140 nm, but significantly smaller islands are also present. Dome islands (marked "*X*") are surrounded by characteristic "capture zones" free of other islands. Comparing images 1(A) and 1(B), recorded at Si coverages $\Theta = 0$ and 4.6 ML, respectively, we see that the base area of larger hut islands as well as of domes increases with Si deposition. Smaller huts, on the other hand, shrink rapidly and disappear at this very initial stage of Si deposition. A striking new feature, clearly visible in images 1(C) and 1(D), appears after deposition of about 6 ML of Si: the islands develop a planar region with (100) orientation at the apex; i.e., the initial pyramid or dome shape of the islands changes to incorporate a (100) top facet, which expands with further Si deposition.

To quantify the changes at the periphery and the apex of the islands upon Si deposition, we measured the evolution in the area of the base and of the top facet for a large number of islands. Figure 2(a) shows results for pyramids and domes. The qualitative observations of Fig. 1—the formation and rapid expansion of a (100) oriented facet at the island top along with a continuous increase in base area during Si growth—are clearly confirmed.

In discussing the results of Figs. 1 and 2(a), we focus on hut islands. We first consider the formation of a (100) facet in the apex region. The reduced height of embedded relative to as-grown 3D SiGe islands observed by XTEM [5] suggests that actual dissolution of the apex plays a role in the formation of this facet. We can demonstrate that this dissolution is driven by the deposition of Si onto the SiGe islands. As-grown islands are stable against shape changes, if they are simply annealed at 650 °C without a Si flux. This result is not surprising, as the islands were formed at significantly higher temperature. If we deposit Si, a top (100) facet forms. Yet if we interrupt the Si flux, the (100) facet does not grow further. For example, we deposited Si onto the islands to a coverage of $\Theta = 7$ ML, somewhat beyond the point at which the formation of a (100) top facet can first be detected by LEEM, stopped the deposition, and annealed at the growth temperature. The (100) facet did not expand. We can thus conclude that a continuous Si flux is required to drive the shape change. The increase in base area of larger huts with Si deposition seen in Figs. 1 and 2(a) can be accounted for by assuming that supplied Si as well as material from the dissolving apex is redistributed such as to preserve the (105) facets of the hut islands as long as possible. Contrary to conclusions reached on other systems [4], our data do not support the idea of directed diffusion of Si atoms from the islands towards the planar wetting layer [12]: the supplied Si sticks on the facets bounding the islands and drives their lateral expansion.

We suggest the following scenario for the dissolution of the island apex. At typical molecular beam epitaxy (MBE) or chemical vapor deposition (CVD) substrate temperatures and growth rates, Si deposition on the (100) [and presumably also (105)] surface of Ge or of a SiGe alloy causes intermixing, i.e., incorporation of Si into and segregation of Ge to the surface to lower the surface energy [13], and to minimize the stress in subsurface layers

[14]. The net effect of this change towards a more Si-rich composition should be most pronounced at the apex of the 3D islands, where the local surface-to-volume ratio is largest. If enough Si is present, the strain in the apex region can become low enough that the (105) facets cannot be maintained and that a (100) surface again becomes the thermodynamically stable structure. Atoms from the apex migrate down the sides to eliminate the (105) facets at the top and promote the outward growth of the remaining (105) facets in the lower parts of the island. The (100) oriented top terraces exposed during the dissolution of the apex are initially Ge rich. Further decay of these terraces, i.e., further reduction of the island height, requires additional intermixing with Si supplied by a continuous Si flux onto the surface, to agree with our observations. For smaller islands with a size close to the critical nucleus, the strain reduction at small Si coverage can already be sufficient to destabilize the entire 3D island. Hence, small islands should disappear at the initial stage of Si deposition, as is indeed observed in Fig. 1. In addition to causing a change in island *shape*, embedding can thus also narrow the distribution of island *sizes*.

We can translate the above model into a simple calculation. Consider an island with a small top terrace "*A*" and whose sides consist of regularly spaced steps [microscopically, the (105) facet consists of close-lying steps [8], as shown in Fig. 2(b)]. We assume that the top of a 3D island is destabilized continuously by mixing with deposited Si and thus decays one atomic layer at a time, i.e., by atom detachment from the topmost monolayer such that its area decreases at a constant rate r. While the actual decay of the apex may involve several layers simultaneously, we expect the respective topmost (smallest) terrace to have highest vapor pressure of its edge atoms, causing it to shrink fastest. Layer-by-layer dissolution may thus be a good approximation. The deposition of Si is also taken into account by defining a second parameter, the fraction p of atoms adsorbed on a monolayer terrace (such as "*A*") that become incorporated into its bounding steps, and thus oppose the island decay. Using this model, we calculate numerically the evolution of the island height and top facet area as a function of Si coverage. The results of this calculation are given as lines in Fig. 2(a), with the two parameters r and p chosen to fit the measured size evolution of the top facet. The data for huts suggest a decay rate $r = 33\ \mathrm{nm}^2/\mathrm{s}$, only slightly smaller than that of isolated monolayer islands on Si(100) at the same temperature [15]. The value found for the second parameter, the step incorporation probability p, is also reasonable: 16% of the adatoms attempting to diffuse across an atomic step become incorporated in it. The calculated curves in Fig. 2(a) clearly demonstrate how dissolution and growth counteract each other. The initially small top terrace of the 3D islands collects only a few Si atoms, yet enough become incorporated into the apex region to make it thermodynamically unfavorable to have (105) facets. Lateral evaporation of the terrace by atom detachment dominates over growth by the incorporation of deposited atoms. This imbalance leads to the removal of material from the apex, causing the island height to decrease. In the calculation this decay of the apex is represented by the increase in the top facet area. Even though the thermodynamic destabilization continues for all exposed (100) terraces in the presence of a Si flux, there is a kinetic limit to the decay of the island: with increasing area of the (100) facet, its lateral growth due to the deposition accelerates and eventually outweighs the decay. Further Si deposition (at the same rate) results in a net expansion of the top facet without additional decrease in island height, and eventual embedding of the 3D island.

The combination of thermodynamic driving force and kinetic limitation suggests that the shape transformation should be temperature and flux dependent. Both our LEEM data and our XTEM results show that Si deposition at low temperature causes only a minor height reduction and a small (100) facet to form on top of the 3D islands: the resulting embedded islands differ only a little from the hut islands. Figure 3 illustrates the evolution of island shape with Si coverage at different temperatures, calculated using our model and starting with an as-grown (105) faceted hut island. We keep the incorporation probability p fixed at the value determined from the fit to the LEEM data, while we vary the rate, r, of detachment. Figure 3 is in good qualitative agreement with our experimental observations. Deposition at low temperature causes little shape change, while at high temperature, it causes the decay of a large portion of the height of the islands, redistribution of larger amounts of SiGe alloy from the apex to the expanding facets, and consequently the transformation of the pyramids into thin, boxlike clusters. We conclude that, because the shape

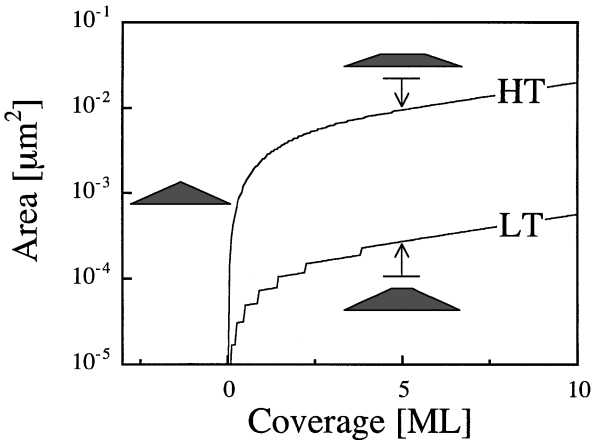

FIG. 3. Calculated top facet area on a 3D island as a function of Si coverage at high and low temperature. The as-grown 3D island is assumed to be a (105) faceted, square based pyramid (base size 140 nm). The resulting shape after the initial stage of Si overgrowth is shown schematically for capping at low (LT) and high (HT) temperature.

change is driven by the thermodynamic destabilization of the apex region through intermixing and a reduction in strain while kinetics limit the actual decay of the island apex, rapid embedding at low temperature preserves the initial hut shape, while slow embedding at higher temperatures causes the 3D islands to flatten maximally, or to disappear entirely if they are small enough. Because of the difference in height reduction, the amount of matrix material required to cover the islands will depend on temperature and flux. We believe that, through judicious choice of growth parameters, specified shapes and heights of 3D islands are achievable and that the electronic properties of individual dots as well as the nature of their coupling can thus be tuned during growth of the embedding layer.

In conclusion, we have investigated embedding of self-assembled 3D SiGe islands in Si *in situ* and in real time by LEEM. Si deposition drives significant changes in the morphology of the islands. Small islands shrink and disappear. Larger islands grow and develop a (100) top facet during the initial stage of Si deposition. These transitions are driven by the Si-induced destabilization of the (105) faceted island apex, followed by the formation of the stable (100) surface by migration. Kinetics ultimately limit the evolution of this process as the flattened islands become buried.

This work was supported by ONR, NSF, and the Swiss National Science Foundation. Expert TEM measurements by E. Mateeva and helpful discussions with Feng Liu and J. Tersoff are gratefully acknowledged.

[1] D. J. Eaglesham and M. Cerullo, Phys. Rev. Lett. **64**, 1943 (1990).

[2] D. Leonard, M. Krishnamurty, C. M. Reaves, S. P. Denbaars, and P. M. Petroff, Appl. Phys. Lett. **63**, 3203 (1993); C. Teichert, M. G. Lagally, L. J. Peticolas, J. C. Bean, and J. Tersoff, Phys. Rev. B **53**, 16 334 (1996).

[3] L. W. Wang and A. Zunger, in *Semiconductor Nanoclusters: Studies in Surface Science and Catalysis*, edited by P. V. Kamat and D. Meisel (Elsevier, Amsterdam, 1996).

[4] Shape changes during capping of InAs islands were reported by X. W. Lin, J. Washburn, Z. Lilienthal-Weber, E. R. Weber, A. Sasaki, A. Wakahara, and Y. Nabetani, Appl. Phys. Lett. **65**, 1677 (1994). Overgrowth of InAs islands was studied by Q. Xie, P. Chen, and A. Madhukar, Appl. Phys. Lett. **65**, 2051 (1994), with emphasis on flattening of the matrix surface.

[5] E. Mateeva, P. Sutter, J. C. Bean, and M. G. Lagally, Appl. Phys. Lett. **71**, 3233 (1997).

[6] J. M. Garcia, G. Medeiros-Ribeiro, K. Schmidt, T. Ngo, J. L. Feng, A. Lorke, J. Kotthaus, and P. M. Petroff, Appl. Phys. Lett. **71**, 2014 (1997).

[7] Islands with Ge concentration $0.2 \leq x \leq 1$ show the same qualitative behavior during embedding. Islands with $x = 0.4$ have an ideal size for observation by LEEM.

[8] Y.-W. Mo, D. E. Savage, B. S. Swartzentruber, and M. G. Lagally, Phys. Rev. Lett. **65**, 1020 (1990).

[9] G. Medeiros-Ribeiro, A. M. Bratkovski, T. I. Kamins, D. A. A. Ohlberg, and R. S. Williams, Science **279**, 353 (1998).

[10] The morphology of individual islands was determined by dark-field LEEM imaging. Use of a diffraction spot resulting from (105) facets allowed the identification of surfaces covered by such facets.

[11] A. J. Steinfort, P. M. L. O. Scholte, A. Ettema, F. Tuinstra, M. Nielsen, E. Landemark, D.-M. Smilgies, R. Feidenhans'l, G. Falkenberg, L. Seehofer, and R. L. Johnson, Phys. Rev. Lett. **77**, 2009 (1996).

[12] N. N. Ledentsov, V. A. Shchukin, M. Grundmann, N. Kirstaedter, J. Böhrer, O. Schmidt, D. Bimberg, V. M. Ustinov, A. Yu. Egorov, A. E. Zhukov, P. S. Kop'ev, S. V. Zaitsev, N. Yu. Gordeev, Zh. I. Alferov, A. I. Borokov, A. O. Kosogov, S. S. Ruvimov, P. Werner, U. Gösele, and J. Heydenreich, Phys. Rev. B **54**, 8743 (1996).

[13] R. M. Tromp, Phys. Rev. B **47**, 7125 (1993); A. J. Hoeven, J. Arts, and P. K. Larsen, J. Vac. Sci. Technol. A **7**, 5 (1989); S. J. Jenkins and G. P. Srivasta, Phys. Rev. B **57**, 8794 (1998).

[14] P. C. Kelires and J. Tersoff, Phys. Rev. Lett. **63**, 1164 (1989).

[15] N. C. Bartelt, W. Theis, and R. M. Tromp, Phys. Rev. B **54**, 11 741 (1996).